

Charge-ordered states in $(\text{La,Sr})_2\text{NiO}_4$ for hole concentrations $n_h = \frac{1}{3}$ and $\frac{1}{2}$

S.-W. Cheong, H. Y. Hwang,* C. H. Chen, B. Batlogg, L. W. Rupp, Jr., and S. A. Carter
AT&T Bell Laboratories, Murray Hill, New Jersey 07974

(Received 21 October 1993)

Real-space ordering of doped holes in $\text{La}_{2-x}\text{Sr}_x\text{NiO}_4$ is revealed in magnetic and electronic-transport anomalies at low temperatures. The ordering is most pronounced for a hole concentration n_h of $\frac{1}{3}$ below 235 K where a superlattice with a modulation wave vector δ of $\frac{1}{3}$ has been found. For $n_h = \frac{1}{2}$, another charge-ordered state with $\delta=0$ is also indicated below ~ 340 K. Our results are, furthermore, suggestive of mesoscopic hole segregation for $0.2 \leq x \leq 0.4$ forming the $n_h = \frac{1}{3}$ and $\delta = \frac{1}{3}$ state below 235 K.

The late transition-metal oxides such as nickelates and cuprates belong to the class of charge-transfer insulators, characterized by an oxygen $2p$ -like valence band and a $3d$ -like upper Hubbard conduction band which results from the strong correlation among the $3d$ electrons.¹ When hole carriers are introduced into these charge-transfer insulators, the holes predominantly have oxygen $2p$ character and interact with $3d$ spins. For instance, the hole could form a spin singlet with the $3d$ spin, the Zhang-Rice singlet,² and/or induce a ferromagnetic interaction between nearest-neighbor $3d$ spins while $3d$ spins, otherwise, couple with each other antiferromagnetically.³ The unconventional dynamics of hole carriers in layered cuprates such as $(\text{La,Sr})_2\text{CuO}_4$ is well reflected in their peculiar normal-state properties and high- T_c superconductivity.⁴

It is intriguing that even though both compounds are charge-transfer oxides, the nature of doped holes in $(\text{La,Sr})_2\text{NiO}_4$ is remarkably different from that in isostructural $(\text{La,Sr})_2\text{CuO}_4$.⁵ It has been proposed theoretically that the influence of electron-phonon (e - p) coupling is more important in the nickelate. If the doped holes localize and distort the lattice locally, energy is gained by the splitting of the degeneracy between the lower Hubbard band of Ni d states and the oxygen $2p$ -like band.^{6,7} In the cuprate, the oxygen $2p$ -like band is higher in energy than that of the lower Hubbard band of Cu d states so that e - p coupling may not play an important role. The large magnetic coupling between Ni and hole spins, in addition to the large e - p coupling, tends to induce self-localization of holes in $(\text{La,Sr})_2\text{NiO}_4$ (Refs. 6 and 8) (herein, we call the self-localized states *small polarons* since e - p coupling is involved).

Recently, we reported the diffraction evidence of *quasi-two-dimensional, mesoscopic charge modulations* at low temperatures with predominant modulation vector $\delta \approx \frac{1}{3}$ (for $0.1 \leq x \leq 0.4$) and 0 (for $x = \frac{1}{2}$) in $\text{La}_{2-x}\text{Sr}_x\text{NiO}_4$ and proposed the model of small polaron ordering.⁹ The unit modulation wave vector δ spans from (π, π) to $(2\pi, 0)$ or $(0, 2\pi)$. According to this observation, the small polaron lattice with $\delta=0$ would consist of small polarons ordered around every other Ni. The $\delta = \frac{1}{3}$ lattice can be pictured from the $\delta=0$ lattice by removing every third diagonal polaron line. We, here, report comprehensive measurements of magnetic and

electronic-transport properties in $\text{La}_{2-x}\text{Sr}_x\text{NiO}_4$. We have discovered distinctive physical anomalies at $x = \frac{1}{3}$ and $x = \frac{1}{2}$, and have observed new phase transitions at 235 K for $x = \frac{1}{3}$ and ~ 340 K for $x = \frac{1}{2}$. These results, together with additional electron-diffraction data, demonstrate that the $x = \frac{1}{3}$ state below 235 K and the $\frac{1}{2}$ state below ~ 340 K are directly associated with the superlattice peaks with $\delta = \frac{1}{3}$ and 0, respectively. These magnetic and transport properties provide strong direct evidence in favor of *small polaron lattices* at low temperatures. Evidence of mesoscopic hole segregation will also be discussed.

The polycrystalline specimens of $\text{La}_{2-x}\text{Sr}_x\text{NiO}_4$ with 17 different compositions between $x=0$ and $x=1$ and $\text{La}_{2-x}(\text{Ba or Ca})_x\text{NiO}_4$ with $x=0.2$ and 0.33 were synthesized by conventional solid-state reaction in air. The sintering with frequent intermediate regrinding was performed in the temperature range of 1150 and 1350°C for three days and the samples were cooled at the rate of 100°C per hour after the final sintering. The chemical issue of cation deficiency or oxygen nonstoichiometry can be quite complex in nickelates such as $\text{Ni}_{1-\delta}\text{O}$ or $\text{La}_2\text{NiO}_{4+\delta}$.^{10,11} To address the oxygen content issue, the specimens were subject to various oxygen treatments such as inert gas annealing or treatment in 200-bar oxygen. We have found that the as-prepared specimens exhibit the cleanest physical properties, in particular, the sharpest phase transition (see below). This observation is consistent with a previous study reporting that the oxygen content of as-prepared $\text{La}_{2-x}\text{Sr}_x\text{NiO}_4$ tends to be stoichiometric for $0.2 \leq x \leq 1$.¹² In this report, we, therefore, emphasize the results on the as-prepared specimens with $x \geq 0.2$.

Displayed in Fig. 1 is the temperature dependence of the resistivity ρ up to 1050 K for representative Sr concentrations. $\rho(T)$ at high temperatures was found to be insensitive ($< 5\%$) to the atmosphere such as air, O_2 , or N_2 , insuring that the high-temperature $\rho(T)$ is intrinsic. The trend of $\rho(T)$ for $x=0.2$ exhibits a semiconductor-like behavior below room temperature and a very weak metalliclike behavior above ~ 600 K. The general trend remains roughly the same with increasing Sr concentration up to $x=0.5$. Beyond $x=0.5$, $\rho(T)$ drops rapidly and becomes metallic for $x \geq 1$ in the whole temperature

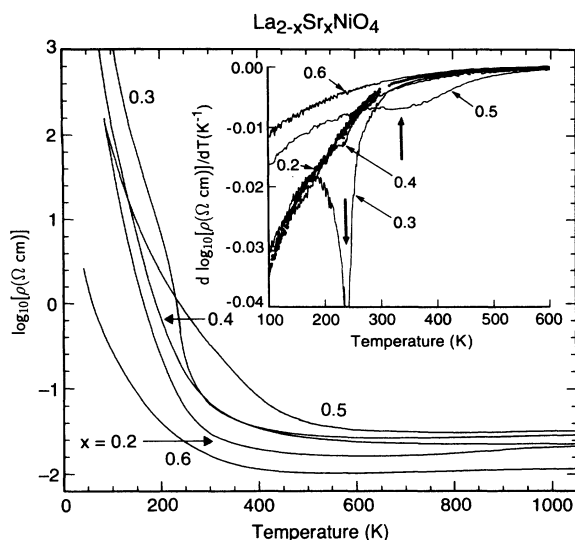


FIG. 1. Logarithmic resistivity as a function of temperature for representative Sr concentrations. The inset displays the temperature derivative of the logarithmic resistivity. Vertical arrows indicate features in the derivative for $x = 0.3$ and 0.5 , indicative of phase transitions.

range.⁵ One striking feature in Fig. 1 is that ρ for $x = 0.3$ increases abruptly at ~ 240 K, indicative of a phase transition. The temperature derivative of $\log_{10}\rho$, plotted in the inset of Fig. 1, shows a sharp dip at 240 K, identifying the phase transition temperature for $x = 0.3$. In the inset, a weak and much broader feature for $x = 0.5$ is also evident at ~ 340 K, suggesting a broad transition for $x = 0.5$.

Magnetic-susceptibility χ measurements were made with various fields up to 50 kOe between 5 and 400 K using a Quantum Design SQUID magnetometer. $\chi(T)$ behaves in a rather complicated way. Spin-glass-like behavior and weak ferromagnetism have been observed below ~ 150 K. However, we found that χ above 200 K is field independent. For representative specimens, $\chi(T)$ between 200 and 300 K, measured while warming in 20 kOe, is shown in the upper panel of Fig. 2. In general, $\chi(T)$ slightly increases below room temperature, but $x = 0.3$ is an exception. For this composition, χ decreases at ~ 240 K where ρ increases abruptly (see Fig. 1), providing an additional indication of a phase transition. As discussed in the following, *this ~ 240 K transition is the most pronounced for $x = \frac{1}{3}$.*

A central result of this study is illustrated in the variation of χ and ρ at 200 K upon Sr substitution as shown in the lower panel of Fig. 2. $\chi(200 \text{ K})$ reaches a local minimum at $x \cong \frac{1}{3}$ and the maximum at $x = \frac{1}{2}$. [In fact, the local minimum of $\chi(200 \text{ K})$ occurs at nominal Sr concentration = 0.32. Since the actual Sr concentration in the ceramic specimens can be slightly different from the nominal concentration and also there may exist a small amount of excess oxygen that can contribute to the hole concentration, we will not distinguish $x = 0.32$, 0.33 , and $\frac{1}{3}$.] A similar, but weaker, trend of $\chi(200 \text{ K})$ vs x also exists even at room temperature as observable in the upper

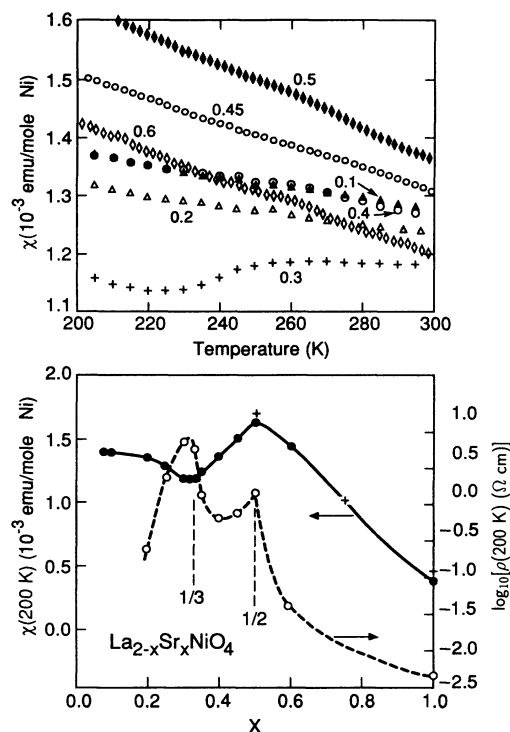


FIG. 2. Upper panel: Susceptibility versus temperature for representative Sr concentrations. Lower panel: susceptibility and logarithmic resistivity at 200 K as a function of Sr doping x . Anomalies at $x = \frac{1}{3}$ and $\frac{1}{2}$ are evident.

panel of Fig. 2. $\rho(200 \text{ K})$ reaches local maxima at $x = \frac{1}{3}$ and $\frac{1}{2}$. ρ above ~ 300 K becomes most insulating at $x = \frac{1}{2}$ as visible in Fig. 1. However, the ρ anomaly at $x = \frac{1}{3}$ is not evident above ~ 300 K. The trend of decreasing ρ and χ upon Sr substitution beyond the $x \approx 0.5$ has been reported.^{5,13} The new result from our careful studies is the discovery of pronounced ρ and χ anomalies at $x = \frac{1}{3}$ and $\frac{1}{2}$.

As exhibited in Fig. 3, the sharp changes of $\rho(T)$ and $\chi(T)$ at approximately 230 K take place for $x = \frac{1}{3}$, independent of divalent ion (Sr, Ba, or Ca) substituted for La. No thermal hysteresis (< 0.5 K) is associated with the changes and $\chi(T)$ drops at the same temperature (< 0.5 K) for fields up to 50 kOe. Thus, the sharp changes of ρ and χ appear to be the result of a *second-order phase transition*. The maximum of ρ and the local minimum of χ at $x = \frac{1}{3}$, shown in the lower panel of Fig. 2, are apparently associated with this phase transition resulting in the increase of $\rho(T)$ and the drop of $\chi(T)$. As shown with arrows in Fig. 3, the phase transition temperature, defined below, for Sr (Ba or Ca) is approximately 235 K (225 K). These results are suggestive that the transition is electronic, rather than simple-structural, in origin and that the hole concentration, not the ionic size of dopant, is the determining factor for the transition.

The extraordinary nature of the phase transition is demonstrated in the temperature derivative of $\log_{10}\rho(T)$ and $\chi(T)/T$ for $\text{La}_{2-x}\text{Sr}_x\text{NiO}_4$ with $0.2 \leq x \leq 0.4$ as plotted in Fig. 4. The peaks in both derivatives, resembling

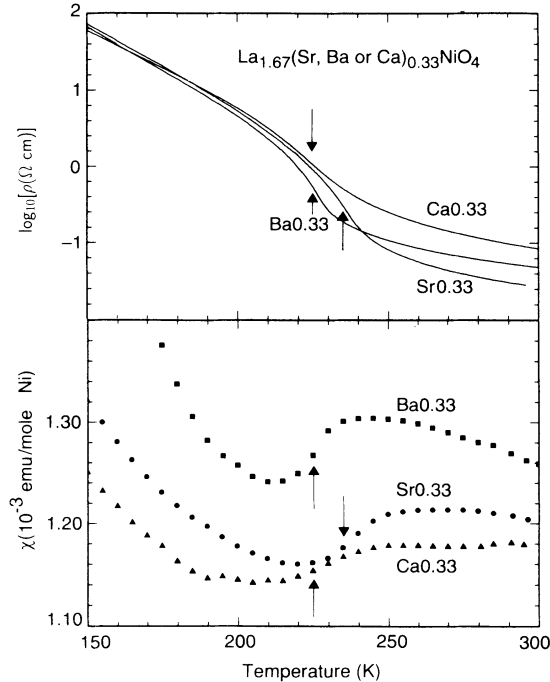


FIG. 3. Logarithmic resistivity (upper panel) and susceptibility (lower panel) as a function of temperature for a fixed concentration ($x = 0.33$) of various divalent dopants (Sr, Ba, or Ca). Arrows indicate phase transition temperatures.

the specific-heat λ anomaly,¹⁴ are the most prominent for $x = \frac{1}{3}$. Furthermore, the phase transition temperatures determined from both derivative peaks are identical and are insensitive (≤ 5 K) to Sr concentration for $0.2 \leq x \leq 0.4$. The results shown in Fig. 4 indicate that the same kind of phase transition occurs at ~ 235 K for $0.2 \leq x \leq 0.4$ and the volume fraction involved in the transition reaches a maximum when x approaches $\frac{1}{3}$. We note that the ~ 340 K ρ anomaly for $x = \frac{1}{2}$, shown in the inset of Fig. 1, exhibits a similar behavior. This ~ 340 K anomaly is weak but clearly visible for $x = 0.48, 0.50$, and 0.52 , becomes even weaker for $x = 0.45$, and absent for $x \leq 0.4$ and $x \geq 0.6$.

The essential experimental findings are the increase of ρ and the drop of χ below the new ~ 235 K phase transition, most pronounced for $x = \frac{1}{3}$. These results could be attributed to the *real-space ordering of the Sr atoms or the doped holes only* without movement of Sr atoms. The first possibility is highly unlikely because a transition temperature of ~ 235 K would require the Sr-La atoms to be mobile at the temperature much lower than the compound formation temperatures ($> 1200^\circ\text{C}$). Our further electron-diffraction work indicates that the volume fraction showing the $\delta \approx \frac{1}{3}$ modulation is the largest for $x \approx \frac{1}{3}$ and the variation of δ from grain to grain for a fixed x is the least for $x = \frac{1}{3}$. Furthermore, the temperature at which the superlattice peaks become visible is in good agreement with the phase transition temperature (~ 235 K) determined from $\rho(T)$ and $\chi(T)$. We, therefore, conclude that the low-temperature state below ~ 235 K for $x \approx \frac{1}{3}$ is characterized by the $\delta = \frac{1}{3}$ superlattice peaks.

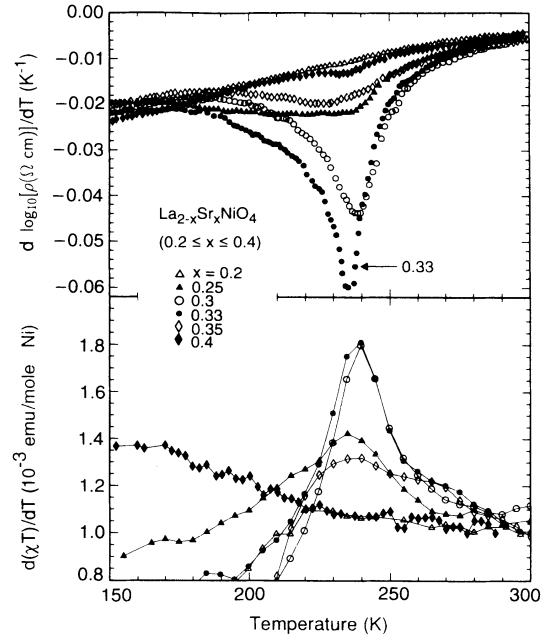


FIG. 4. Temperature derivative of logarithmic resistivity (upper panel) and susceptibility multiplied by temperature (lower panel) versus temperature for Sr concentrations of $0.2 \leq x \leq 0.4$.

The $x = \frac{1}{2}$ state, similarly, is associated with the $\delta = 0$ superlattice peaks. The intensity of the $\delta = 0$ peaks is much weaker than that of the $\delta = \frac{1}{3}$ peaks, indicating that the charge modulation of the $\delta = 0$ state is weaker and/or involves a smaller volume fraction. The $\delta = 0$ peaks are found to exist even at room temperature, again consistent with the ρ feature at ~ 340 K. The order parameter associated with the $\delta = 0$ state appears to be very small, which may be related with the truly two-dimensional nature of the $\delta = 0$ state.⁹

Since the ~ 235 K transition is the most pronounced for $x = \frac{1}{3}$ and the superlattice modulation with $\delta \approx \frac{1}{3}$ is found in a wide Sr range ($0.2 \leq x \leq 0.4$), one may speculate that when x differs from $\frac{1}{3}$ but in the range of $0.2 \leq x \leq 0.4$, *segregation of doped holes* occurs to form the preferred charge-ordered state of hole concentration $n_h = \frac{1}{3}$. Simple Sr chemistry such as Sr inhomogeneity or phase separation of Sr ions can be ruled out as the origin of the phenomena because x-ray diffraction peaks are always sharp and lattice parameters change linearly and rapidly upon Sr substitution.⁹ The issue of oxygen inhomogeneity can be rather complicated. However, since our specimens are nearly oxygen stoichiometric, it is not very plausible that (excess) oxygen alone can account for our observations. The dark field images obtained from the superlattice peaks, in addition to our previous analysis of superlattice peak widths, reveal that the in-plane (out-of-plane) dimension of the charge-ordered region is ~ 500 Å (~ 60 Å). Therefore, the hole segregation for $x \neq \frac{1}{3}$ would break charge neutrality in the intermediate length scale of ~ 500 Å. This mesoscopic breakdown of charge neutrality may be allowed as long as long-range

Coulomb interaction between the holes and lattice is sufficiently weak, i.e., if the background dielectric constant is large enough. It is also conceivable that the charge imbalance produced by the hole segregation may be compensated by the mesoscopic diffusion of counterions such as oxygen. Similar hole segregation has been extensively discussed for doped antiferromagnets in conjunction with superconducting layered cuprates. It has been theoretically shown that dilute holes in a layered antiferromagnet can be unstable against phase separation into hole-rich and hole-poor regions at intermediate length scales.¹⁵ This hole phase separation arises from clustered holes breaking fewer antiferromagnetic bonds than randomly distributed holes do.¹⁵

Our results share somewhat similar nature with the Verwey transition in magnetite Fe_3O_4 .¹⁶ Similar to that of $(\text{La,Sr})_2\text{NiO}_4$, ρ in Fe_3O_4 shows a broad minimum at ~ 350 K with slow increase above ~ 350 K and fast increase below ~ 350 K and a discontinuous jump at the Verwey transition (~ 125 K) by two orders of magnitude. The resistivity of Fe_3O_4 above ~ 125 K was attributed to a superposition of band and hopping conduction of small polarons.¹⁷ In the Verwey model, carriers undergo an order-disorder transition at ~ 125 K. It turns out that the actual charge ordering, estimated from various diffraction data, is much more complicated than the Verwey model.¹⁸ Major difficulty in understanding the Verwey transition lies in the structural complexity.¹⁹

The existing theoretical and experimental evidences of small polarons^{6,8} lead to the obvious possibility that the charge ordering in $(\text{La,Sr})_2\text{NiO}_4$ is the result of the for-

mation of small polaron lattices.⁹ Interestingly, ρ in $(\text{La,Sr})_2\text{NiO}_4$ can be qualitatively explained within the framework of small polaron conduction. As in Fe_3O_4 ,¹⁷ the tendency of slow ρ increase at high temperatures may be due to band conduction of small polarons and the rapid semiconductorlike increase of ρ at low temperatures can be ascribed to hopping conduction of small polarons. Since the polaron-ordered regions with the in-plane dimension of ~ 500 Å are expected to be highly resistive, conductivity at low temperatures, even below the polaron-ordering temperatures, is probably dominated by the percolative conduction through the polaron-disordered regions. This percolative conduction would explain why the temperature dependence of ρ is rather insensitive to Sr concentration for $x \leq 0.5$.

Our extensive investigation on $(\text{La,Sr})_2\text{NiO}_4$ leads to the conclusion that charge-ordered states exist at low temperatures; one corresponds to $n_h = \frac{1}{3}$ and $\delta = \frac{1}{3}$ and another to $n_h = \frac{1}{2}$ and $\delta = 0$. We propose that segregation of hole carriers occurs for $0.2 \leq x \leq 0.4$ in such a way as to form mesoscopic domains (~ 500 Å) of the $n_h = \frac{1}{3}$ and $\delta = \frac{1}{3}$ state below ~ 235 K. Our discoveries in the layered nickelates where electron-phonon coupling plays an important role further reveal the exceedingly rich nature of charge dynamics in charge-transfer oxides, already manifested in the superconductivity in layered cuprates.

We thank P. B. Littlewood and J. Zaanen for enlightening discussions.

*Present address: Department of Physics, Princeton University, Princeton, NJ 08540.

¹J. Zaanen, G. A. Sawatzky, and J. W. Allen, Phys. Rev. Lett. **55**, 418 (1985).

²F. C. Zhang and T. M. Rice, Phys. Rev. B **37**, 3759 (1988).

³A. Aharony et al., Phys. Rev. Lett. **60**, 1330 (1988).

⁴For a review, see, for example, B. Batlogg, Physica (Amsterdam) **169B**, 7 (1990); or P. W. Anderson, Science **256**, 1526 (1992).

⁵R. J. Cava et al., Phys. Rev. B **43**, 1229 (1991).

⁶V. I. Anisimov et al., Phys. Rev. Lett. **68**, 345 (1992).

⁷Z. Tan et al., Phys. Rev. B **47**, 12 365 (1993).

⁸X.-X. Bi and P. C. Eklund, Phys. Rev. Lett. **70**, 2625 (1993).

⁹C. H. Chen, S.-W. Cheong, and A. S. Cooper, Phys. Rev. Lett. **71**, 2461 (1993).

¹⁰C. M. Osburn and R. W. Vest, J. Phys. Chem. Solids **32**, 1331 (1971).

¹¹J. M. Tranquada, D. J. Buttrey, and D. E. Rice, Phys. Rev. Lett. **70**, 445 (1993).

¹²X. Granados et al., J. Solid State Chem. **102**, 455 (1993).

¹³Y. Takeda et al., Mater. Res. Bull. **25**, 293 (1990).

¹⁴M. E. Fisher, Philos. Mag. **7**, 1731 (1962); M. E. Fisher and J. S. Langer, Phys. Rev. Lett. **20**, 665 (1968); Y. Suezaki and H. Mori, Prog. Theor. Phys. **41**, 1177 (1969).

¹⁵V. J. Emery, S. A. Kivelson, and H. Q. Lin, Phys. Rev. Lett. **64**, 475 (1990); V. J. Emery and S. A. Kivelson, Physica C **209**, 597 (1993).

¹⁶E. J. W. Verwey and P. W. Haaymann, Physica **8**, 979 (1941); for a review, see, for example, N. Tsuda, K. Nasu, A. Yanase, and K. Siratori, *Electronic Conduction in Oxides* (Springer-Verlag, Berlin, 1991), p. 207.

¹⁷L. Degiorgi, P. Wachter, and D. Ihle, Phys. Rev. B **35**, 9259 (1987).

¹⁸Y. Yamada, N. Wakabayashi, and R. M. Nicklow, Phys. Rev. B **21**, 4642 (1980).

¹⁹See, for example, J. Yoshida and S. Iida, J. Phys. Soc. Jpn. **47**, 1627 (1979).